

Construction of a cuproptosis-associated long non-coding RNA risk prediction model for pancreatic adenocarcinoma based on the TCGA database

Wenguang Cui, Postgraduate^{a,*} , Yaling Wang, Professor^b, Jianhong Guo, Postgraduate^a, Zepeng Zhang, Postgraduate^a

Abstract

Cuproptosis is a recently identified controlled process of cell death that functions in tumor development and treatment. Long non-coding RNAs (lncRNAs) are RNA molecules longer than 200 nucleotides that bind to transcription factors and regulate tumor invasion, penetration, metastasis, and prognosis. However, there are limited data on the function of cuproptosis-associated lncRNAs in pancreatic adenocarcinoma. Utilizing data retrieved from the cancer genome atlas database, we devised a risk prediction model of cuproptosis-associated lncRNAs in pancreatic adenocarcinoma, determined their prognostic significance and relationship with tumor immunity, and screened potential therapeutic drugs. Overall, 178 patients were randomized to a training or test group. We then obtained 6 characteristic cuproptosis-associated lncRNAs from the training group, based on which we constructed the risk prediction model, calculated the risk score, and verified the test group results. Subsequently, we performed differential gene analysis, tumor immunoassays, functional enrichment analysis, and potential drug screening. Finally, we found that the prediction model was highly reliable for the prognostic assessment of pancreatic adenocarcinoma patients. Generally, low risk patients had better outcomes than high risk patients. A tumor immunoassay showed that immunotherapy may benefit high risk patients more as there is a greater likelihood that the tumors could escape the immune system in low-risk patients. Through drug screening, we identified ten drugs that may have therapeutic effects on patients with pancreatic adenocarcinoma. In conclusion, this study constructed a risk prediction model of cuproptosis-associated lncRNAs, which can reliably predict the prognosis of pancreatic adenocarcinoma patients, provided a clinical reference for determining treatment approach, and provided some insights into the associations between lncRNAs and cuproptosis. This provides useful insight to aid in the development of therapeutic drugs for pancreatic adenocarcinoma.

Abbreviations: C-index = consistency index, DEGs = differentially expressed genes, FDX1 = Ferredoxin 1, ICIs = immune checkpoint inhibitors, LASSO = least absolute shrinkage and selection operator, lncRNA = long non-coding RNA, OS = overall survival, PFS = progression free survival, ROC = receiver operating characteristic, ssGSEA = single sample gene set enrichment analysis, TCGA = the cancer genome atlas, TIDE = tumor immune dysfunction and exclusion, TMB = tumor mutation burden.

Keywords: cuproptosis, lncRNA, pancreatic adenocarcinoma, prediction model, TCGA database

1. Introduction

Pancreatic adenocarcinoma is a malignant, invasive gastrointestinal cancer with a 5-year survival rate of under 8%.^[1,2] According to a report published by the National Cancer Center of China in 2016, there is an increasing incidence of pancreatic adenocarcinoma in China and the mortality rate is ranked 7th.^[3] The early clinical symptoms of the disease are occult, and

it progresses rapidly. Most patients show local progression or distal metastasis upon diagnosis. Even with surgical resection, the vast majority of patients will relapse. Therefore, there is a need for new prognostic indicators and a reliable and effective prediction system in order to improve the clinical prognosis of pancreatic adenocarcinoma.

Long non-coding RNA (lncRNA) molecules are comprised of over 200 ribonucleotides, and they were originally considered a

Supported by Science and Technology Research and Development Plan of Zhangjiakou, Hebei Province, China (Grant No.1911021D-1).

The authors have no conflicts of interest to disclose.

The datasets generated during and/or analyzed during the current study are publicly available.

Ethics committee or institutional review board approval was not required to approve this study.

Supplemental Digital Content is available for this article.

^a Hebei North University, Zhangjiakou, Hebei Province, China, ^b The First Affiliated Hospital of Hebei North University, Zhangjiakou, Hebei Province, China.

* Correspondence: Wenguang Cui, Hebei North University, No.11, South Diamond Road, Zhangjiakou, Hebei Province 075000, China (e-mail: 763976054@QQ.com).

Copyright © 2023 the Author(s). Published by Wolters Kluwer Health, Inc. This is an open-access article distributed under the terms of the Creative Commons Attribution-Non Commercial License 4.0 (CCBY-NC), where it is permissible to download, share, remix, transform, and buildup the work provided it is properly cited. The work cannot be used commercially without permission from the journal.

How to cite this article: Cui W, Wang Y, Guo J, Zhang Z. Construction of a cuproptosis-associated long non-coding RNA risk prediction model for pancreatic adenocarcinoma based on the TCGA database. *Medicine* 2023;102:5(e32808).

Received: 9 November 2022 / Received in final form: 9 January 2023 / Accepted: 10 January 2023

<http://dx.doi.org/10.1097/MD.00000000000032808>

byproduct of RNA polymerase II transcription. They are important regulators of tumorigenesis and associated with neoplasm invasion, metastasis, and prognosis. An ever-increasing number of lncRNA elements have been discovered, a process which has benefited from the advancement of high-throughput sequencing technologies. Cai et al^[4] found that hox transcript antisense RNA limits insulin-like growth factor 2 inhibition via the miR-663b promoter, promoting proliferation and inhibiting apoptosis in pancreatic cancer cells. In addition, lncRNAs, such as

noncoding RNA activated by DNA damage and X-inactive specific transcript, promote the critical metastatic mechanism epithelial-mesenchymal transition in pancreatic adenocarcinoma cells.^[5-7] However, a small number of lncRNAs can inhibit the occurrence and development of pancreatic adenocarcinomas; in 2013, Lu et al^[8] confirmed that there was reduced expression of a lncRNA called growth arrest specific 5 in pancreatic adenocarcinoma tissue and growth arrest specific 5 overexpression inhibited pancreatic adenocarcinoma cell proliferation.

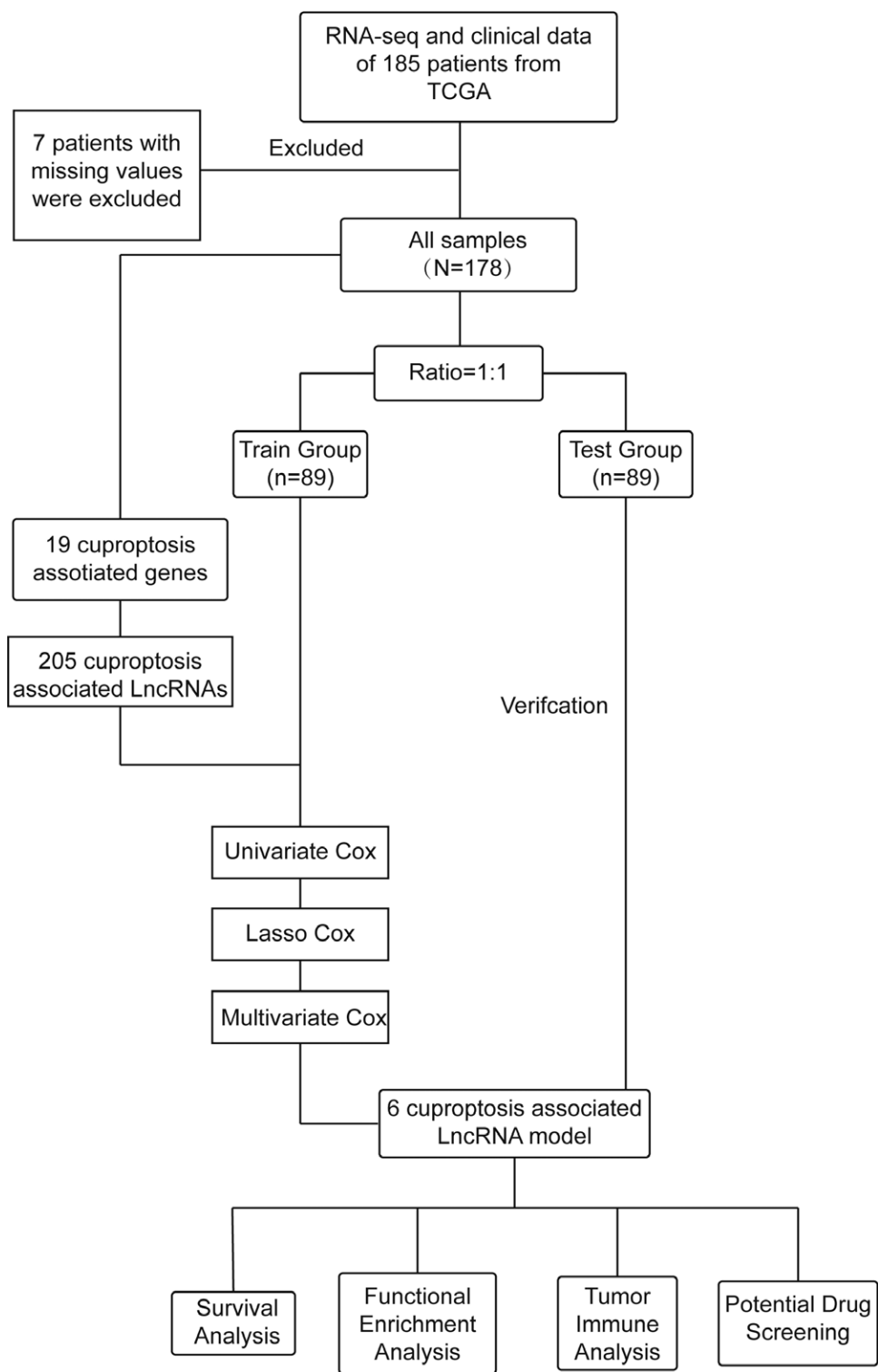


Figure 1. Flowchart of the study.

Tumor development, invasion, and drug resistance occur largely due to defects of cell death pathways in cancer cells. The categories of cell death were previously known to include apoptosis, necroptosis, pyroptosis, and ferroptosis^[9]; however, Tsvetkov et al^[10] proposed another mechanism of cell death in 2019: cuproptosis. In 2022, their research showed^[11] that its mechanism differs from those of the other 4 forms. The process of cuproptosis depends on cellular copper aggregation,^[11] which leads to the accumulation of lipoylated proteins from the tricarboxylic acid (TCA) cycle. This inhibits the TCA cycle, leading to proteotoxic stress and inducing cell death. They also revealed that ferredoxin 1 (FDX1) regulates cuproptosis and protein lipoacylation.^[11]

Data analysis demonstrated that cuproptosis-associated lncRNA signatures could well predict the prognosis of many kinds of cancer.^[12-15] Despite these studies, the function of cuproptosis-associated lncRNAs in pancreatic adenocarcinoma

has not been fully established. To address this gap, we identified cuproptosis-associated lncRNAs in pancreatic adenocarcinoma using the cancer genome atlas (TCGA) database. We built a cuproptosis-associated lncRNA risk prediction model, analyzed its functional enrichment and immune-related functions, explored its possible mechanism, and provided insight for the development of new pharmacological approaches for pancreatic adenocarcinoma.

2. Materials and methods

2.1. Data & identification of cuproptosis-associated lncRNAs

Clinical, tumor mutation burden, and transcriptomic data for 185 pancreatic adenocarcinoma patients were retrieved

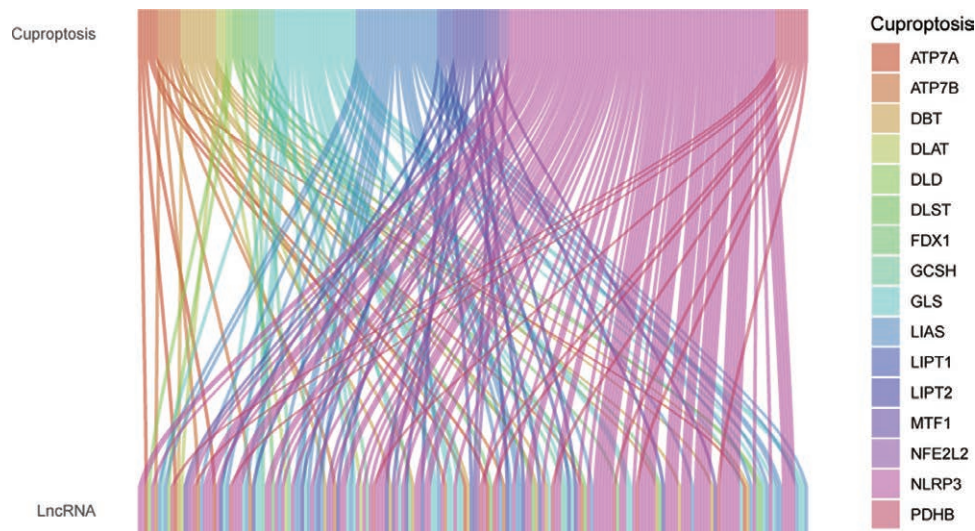


Figure 2. Sankey diagram of 205 cuproptosis associated lncRNAs correlated with 19 cuproptosis associated genes. lncRNA = long non-coding RNA.

Table 1

Baseline clinical characteristic.

	Type	Total	Test	Train	P value
Age	≤65	94 (52.81%)	50 (56.18%)	44 (49.44%)	.4528
	>65	84 (47.19%)	39 (43.82%)	45 (50.56%)	
Gender	Female	80 (44.94%)	44 (49.44%)	36 (40.45%)	.2915
	Male	98 (55.06%)	45 (50.56%)	53 (59.55%)	
Grade	G1	31 (17.42%)	17 (19.1%)	14 (15.73%)	.9435
	G2	95 (53.37%)	47 (52.81%)	48 (53.93%)	
	G3	48 (26.97%)	23 (25.84%)	25 (28.09%)	
	G4	2 (1.12%)	1 (1.12%)	1 (1.12%)	
	Unknow	2 (1.12%)	1 (1.12%)	1 (1.12%)	
	Stage	Stage I	21 (11.8%)	10 (11.24%)	
Stage II	147 (82.58%)	72 (80.9%)	75 (84.27%)		
Stage III	3 (1.69%)	2 (2.25%)	1 (1.12%)		
Stage IV	4 (2.25%)	3 (3.37%)	1 (1.12%)		
Unknow	3 (1.69%)	2 (2.25%)	1 (1.12%)		
T	T1	7 (3.93%)	4 (4.49%)	3 (3.37%)	.7722
	T2	24 (13.48%)	10 (11.24%)	14 (15.73%)	
	T3	142 (79.78%)	71 (79.78%)	71 (79.78%)	
	T4	3 (1.69%)	2 (2.25%)	1 (1.12%)	
	Unknow	2 (1.12%)	2 (2.25%)	0(0%)	
M	M0	80 (44.94%)	44 (49.44%)	36 (40.45%)	.7869
	M1	4 (2.25%)	3 (3.37%)	1 (1.12%)	
	Unknow	94 (52.81%)	42 (47.19%)	52 (58.43%)	
N	N0	49 (27.53%)	26 (29.21%)	23 (25.84%)	.6306
	N1	124 (69.66%)	59 (66.29%)	65 (73.03%)	
	Unknow	5 (2.81%)	4 (4.49%)	1 (1.12%)	

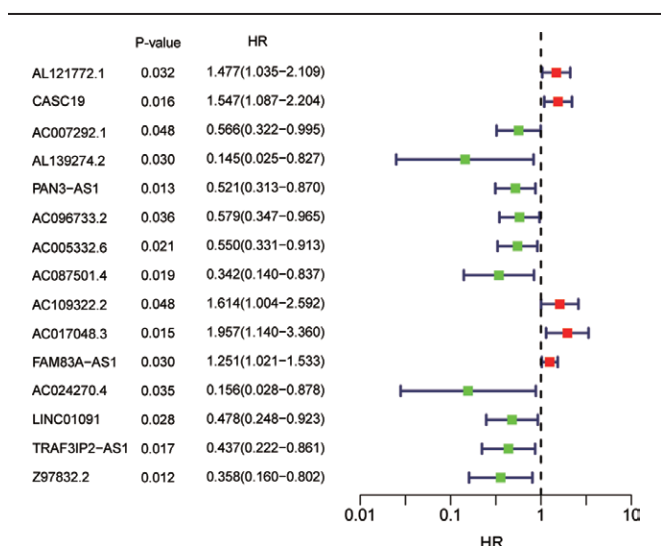


Figure 3. The univariate Cox regression analysis between cuproptosis associated LncRNAs and OS of pancreatic cancer, which was shown in the forest plot. The P-values and Hazard Ratios were obtained by univariate Cox regression. LncRNA = long non-coding RNA, OS = overall survival.

from the TCGA database (<https://portal.gdc.cancer.gov/repository>); details are provided in Supplementary Digital Content 1, Supplemental Digital Content, <http://links.lww.com/MD/I413>. Seven patients were withdrawn due to missing values. Through a literature search, we identified cuproptosis-associated genes. Pearson correlation was used to evaluate the relationship between lncRNAs and cuproptosis-associated genes, after which the cuproptosis-associated lncRNAs were screened for a coefficient > 0.1 ($R > 0.1$), $P < .05$.

2.2. Construction & verification of a risk prediction model

The 178 enrolled patients were randomly assigned to either a training or test group. The research process is illustrated in Figure 1.

For the training group, univariate Cox and least absolute shrinkage and selection operator (Lasso) regressions were used to obtain characteristic cuproptosis-associated lncRNAs. Next, we used multivariate Cox regression to construct a cuproptosis-associated lncRNA risk prediction model for pancreatic adenocarcinoma. We calculated risk scores as: risk score = \sum characteristic cuproptosis-associated lncRNA expression \times correlation coefficient (we kept 4 decimal places).

Training and test groups were categorized as high risk or low risk with the median risk score as a threshold. We compared overall survival (OS) and progression-free survival (PFS) rates between high- and low risk training and test groups using Kaplan–Meier analysis; this was used to investigate whether risk score was predictive of prognosis. The model performance was assessed using consistency index (C-index) and receiver operating characteristic (ROC) curve.

2.3. Differential gene analysis & function enrichment analysis

The differential expression analyses of cuproptosis-associated genes were performed using the R limma package with the screening conditions of a False Detection Rate (FDR) < .05 and $\log_2FC > 1$. We used clusterprofile^[16] in R to perform gene ontology enrichment analysis of cuproptosis-associated differentially expressed genes (DEGs) between risk groups; this included evaluating biological process, cellular component, and molecular function, with screening conditions of a FDR < .05. We also used Kyoto encyclopedia of genes and genomes pathway enrichment analysis, with an FDR < .05.

2.4. Tumor Immunoassay

Based on single-sample gene set enrichment analysis (ssGSEA), we assessed the association between the 6 characteristic cuproptosis-associated lncRNAs and immune function by the gene set variation analysis and GSEABase packages in R.

After obtaining mutation data of the 178 pancreatic adenocarcinoma patients from the TCGA database, we used the maftools package in R for integration with clinical data. Then we used the survminer and ggpubr packages to analyze the differences in

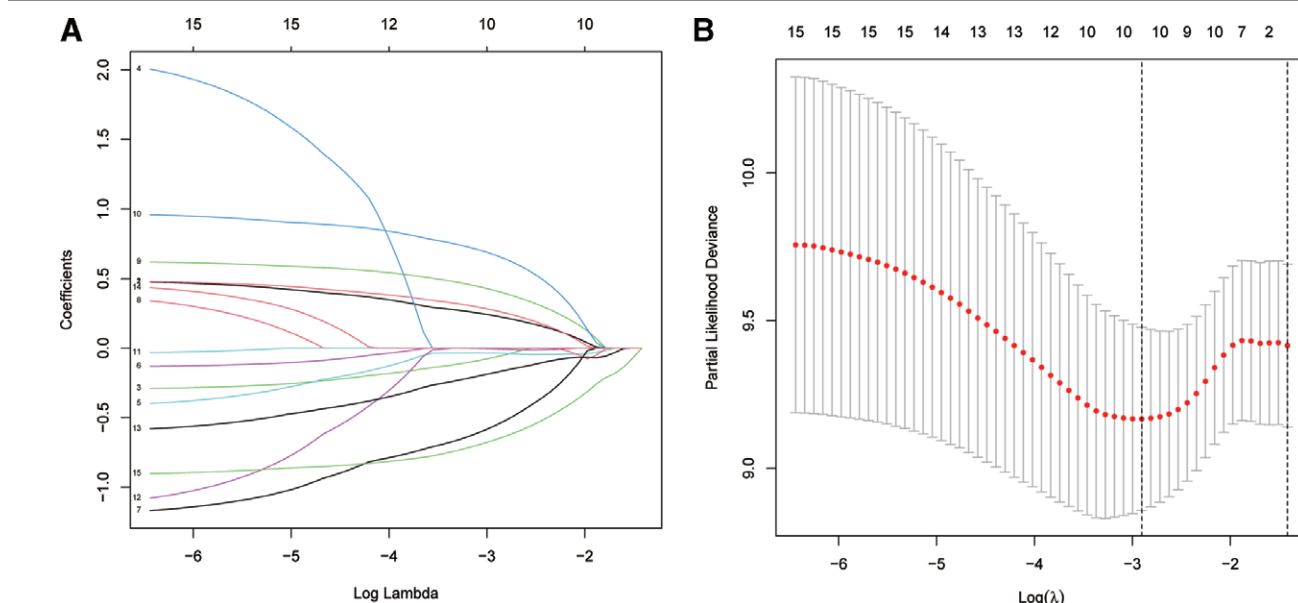


Figure 4. (a) In least absolute shrinkage and selection operator (Lasso) regression, the coefficients of cuproptosis associated LncRNAs were calculated. (b) According to minimum criteria, 10 cuproptosis associated LncRNAs were selected by the Lasso regression. LASSO = least absolute shrinkage and selection operator, LncRNA = long non-coding RNA.

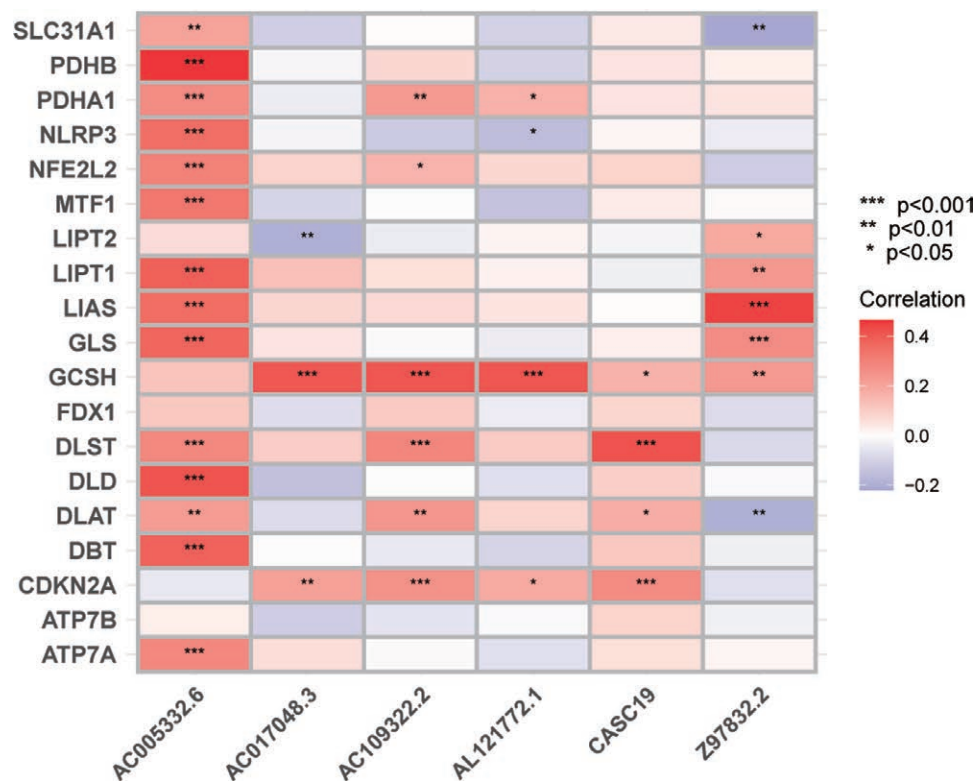


Figure 5. The correlations between cuproptosis associated genes and the 6 prognostic cuproptosis associated lncRNAs in the prognostic model. lncRNA = long non-coding RNA.

tumor mutation burden (TMB) and survival between high-risk and low-risk groups.

The tumor immune dysfunction and exclusion (TIDE) score of enrolled patients was retrieved from the TIDE website (<http://tide.dfc.harvard.edu>) by uploading transcriptomic data of the 178 pancreatic adenocarcinoma patients to the website. Then we assessed potential differences in immunotherapy responses between the low- and high-risk groups using the ggpubr package.

2.5. Potential drug screening

We used the pRRophetic,^[17] cgp2016 database and ggplot2 packages in R to determine each sample half-inhibitory concentration (IC50) to compare drug sensitivity between risk groups and evaluate the effects of drug treatment using Wilcoxon signed-rank test.

2.6. Statistical analysis

Data analysis and graphic visualization were performed using R^[18] version 4.1.3 (<https://www.r-project.org/>). Results were considered significant at $P < .05$.

3. Results

3.1. Identification of cuproptosis-associated lncRNAs

19 cuproptosis-associated genes were identified through a literature search: ATP7B, ATP7A, CDKN2A, DBT, DLD, DLAT, DLST15-19, FDX1, GCSH, GLS, LIAS, LIPT1, LIPT2, MTF1, NFE2L2, NLRP3, PDHA1, PDHB, and SLC31A1.^[11,19-22] Through Pearson correlation analysis, we found that these genes were associated with 205 lncRNAs (Fig. 2).

3.2. Construction & verification of a risk prediction model

The 178 enrolled patients with pancreatic adenocarcinoma were randomized to a training or test group (n = 89 each). The

clinical characteristics were not different ($P > .05$) between groups (Table 1). Clinical data are shown in Supplementary Digital Content 2, Supplemental Digital Content, <http://links.lww.com/MD/I414>.

For the training group, 205 cuproptosis-associated lncRNAs were first analyzed using univariate Cox regression, leading to the identification of 15 cuproptosis-associated lncRNAs that were significantly associated with prognosis (Fig. 3). Lasso regression was conducted to reduce multicollinearity, leaving ten cuproptosis-associated lncRNAs (Fig. 4). Finally, multivariate Cox analysis was performed and identified 6 characteristic cuproptosis-associated lncRNAs that were independent prognostic factors (Fig. 5).

$$\text{Risk score} = \text{AL121772.1} \times 0.3493 + \text{CASC19} \times 0.4448 + \text{A} - 0.8422 + \text{AC109322.2} \times 0.5305 + \text{AC017048.3} \times 0.9961 +$$

45 patients were enrolled in the training group and 44 were enrolled in the low-risk group. Figure 6b, d, and f show the risk status, survival status, and characteristic cuproptosis-associated lncRNA expression of each individual in the training group. The high-risk group had lower OS and PFS than the low-risk group (Figs. 7, 8).

To assess the accuracy of this model, we calculated risk scores for the test group. 27 test group patients and 62 low risk patients were enrolled. Risk status, survival status, and characteristic cuproptosis-associated lncRNA expression levels of each patient in the test group are shown in Figure 6a, 6c, and 6e. The risk groups differed significantly with lower OS and PFS rates for the high-risk group (Figs. 7, 8). The ROC curve produced Area Under the Curve (AUC) values of 0.723 at 1 year, 0.729 at 3 years, and 0.755 at 5 years (Fig. 9a). The clinical ROC curve (Fig. 9b) and C-index curve (Fig. 10) indicated that the prediction model was more successful at evaluating risk prediction than other clinical methods.

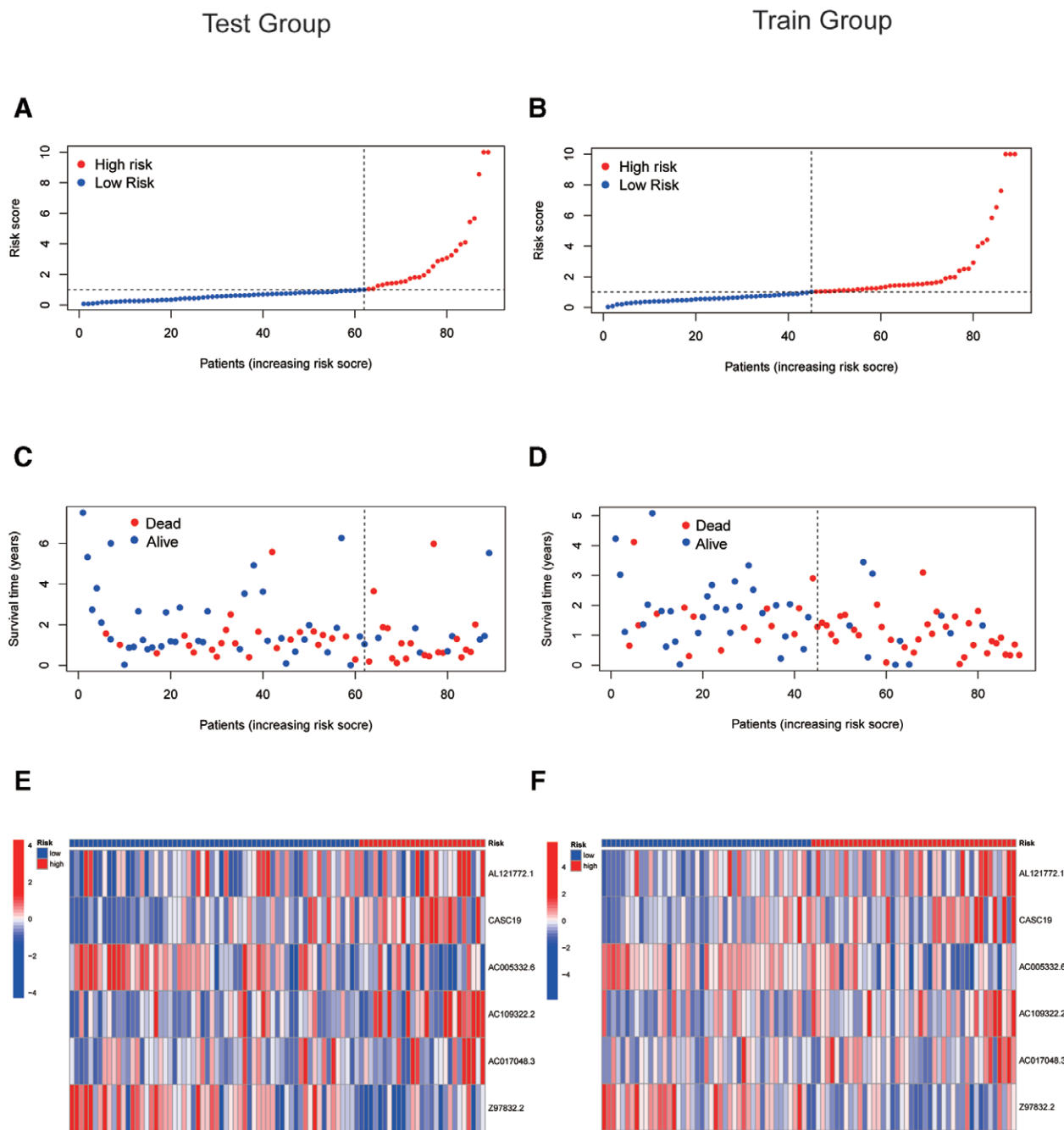


Figure 6. (a)(c)(e) The distribution of the risk scores, survival scatter diagram and expression heatmap of 6 cuproptosis associated lncRNAs in the test group. (b)(d)(f) The distribution of the risk scores, survival scatter diagram and expression heatmap of 6 cuproptosis associated lncRNAs in the train group. lncRNA = long non-coding RNA.

Subsequently, stratified analysis was performed. When stratified by age (> 60 and < 60 years), there were lower survival rates for the high-risk patients than the low-risk patients (Fig. 11a, b) in both age groups. When stratified by sex, high risk males had lower survival rates than low risk males, but there were no significant differences between risk groups for female patients (Fig. 11c, d). When stratified by tumor malignancy, survival rates were lower for high-risk patients with Grade 1 to 2 and 3 to 4 tumors than in low-risk patients (Fig. 11e, f).

Through principal component analysis, we compared the expression of 19 cuproptosis-associated genes, 205 cuproptosis-associated lncRNAs, and 6 characteristic cuproptosis-associated lncRNAs between risk groups. Figure 12 shows wide variation in gene expression between the risk groups.

3.3. Functional enrichment analysis

The gene ontology enrichment analyses determined that cuproptosis-associated DEGs were primarily involved in immune-related biological processes; the cellular components they were associated with were primarily the outer plasma membrane, plasma membrane signaling receptor complex, and T cell receptor complex; their molecular function was related to antigen binding and ion channel activity (Fig. 13). Kyoto encyclopedia of genes and genomes pathway enrichment analyses revealed that DEGs were primarily involved in neuroactive ligand-receptor interactions, cytokine-cytokine receptor interactions, and the cAMP signaling pathway (Fig. 14).

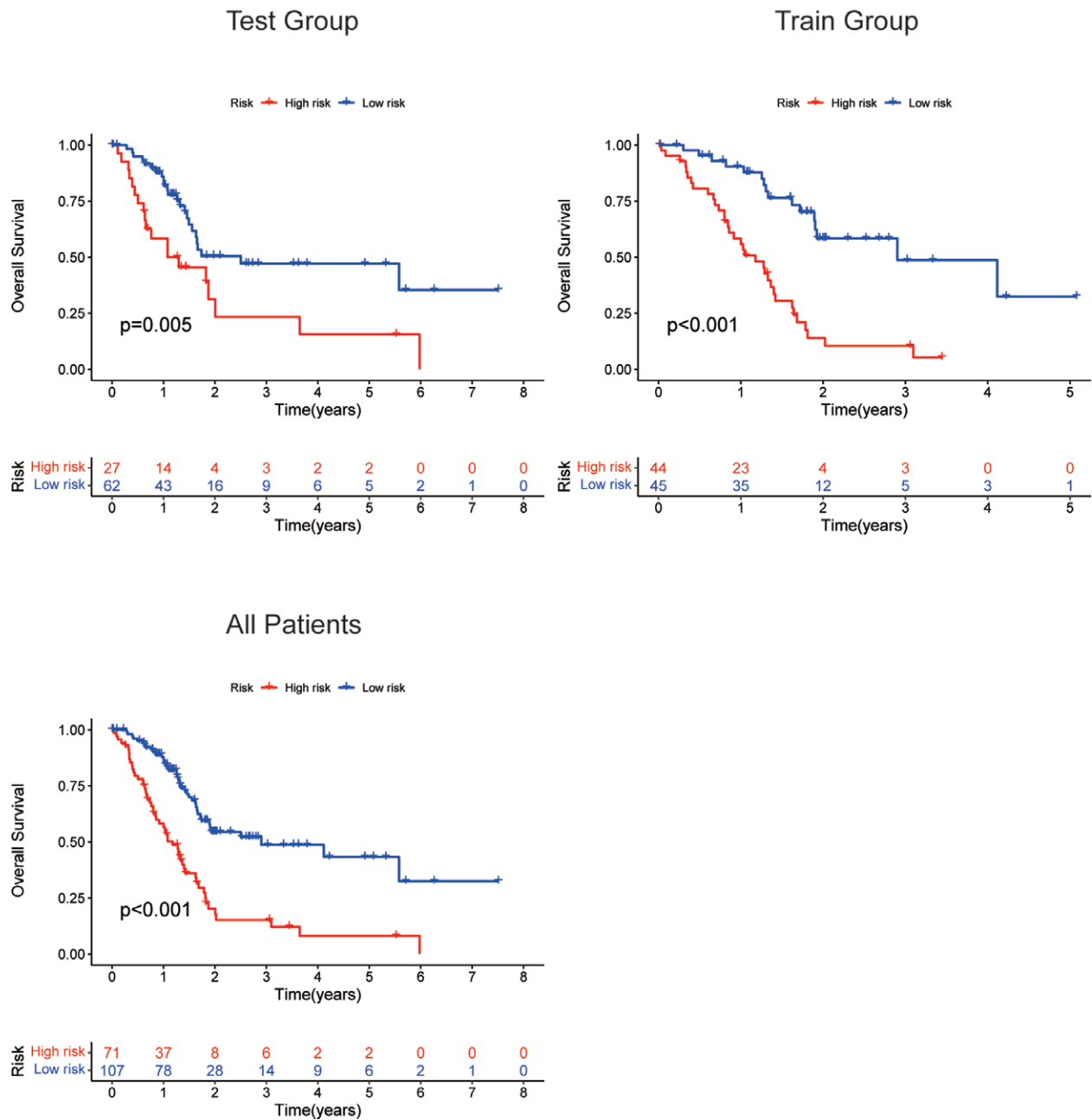


Figure 7. The Kaplan–Meier curves depicting the OS between high-risk and low-risk groups in the test group, train group and all patients. OS = overall survival.

3.4. Tumor immunoassay

Based on ssGSEA, we assessed the association between the 6 characteristic cuproptosis-associated lncRNAs and immune function; the following immune functions showed a considerably greater abundance in the low risk group: chemokine receptor (CCR), type_II_IFN_Response, human leukocyte antigen, cytolytic activity, T_cell_Co_invitation, check_point, and T_cell_Co_stimulation (Fig. 15a).

TMB is a potential predictor of immune checkpoint blockade therapy outcomes. Analysis of mutational data from all patients revealed higher TMB in high risk than low risk patients (Fig. 16c), which suggests that this immunotherapy may be more beneficial for high-risk individuals. In general, survival rates were lower in patients with high TMB (Fig. 16a). The probability of survival was highest in low-risk patients with low TMB, followed by all patients with high TMB; meanwhile, the

probability of survival was lowest in in high risk patients with low TMB (Fig. 16b).

The TIDE web platform can use pretreatment tumor expression as a computational framework to estimate multiple published transcriptomic biomarkers to predict patient responses to immunotherapy. Using the TIDE model for our data, we determined that TIDE and risk score were not correlated (Fig. 15b), and immune evasion was more likely in low-risk patients.

3.5. Potential drug screening

There was a worse prognosis for high-risk patients. To compare drug sensitivity between the risk groups and evaluate the effects of drug treatment, we calculated the IC50 for each individual with the pRRophetic package and cgp2016 database in R.

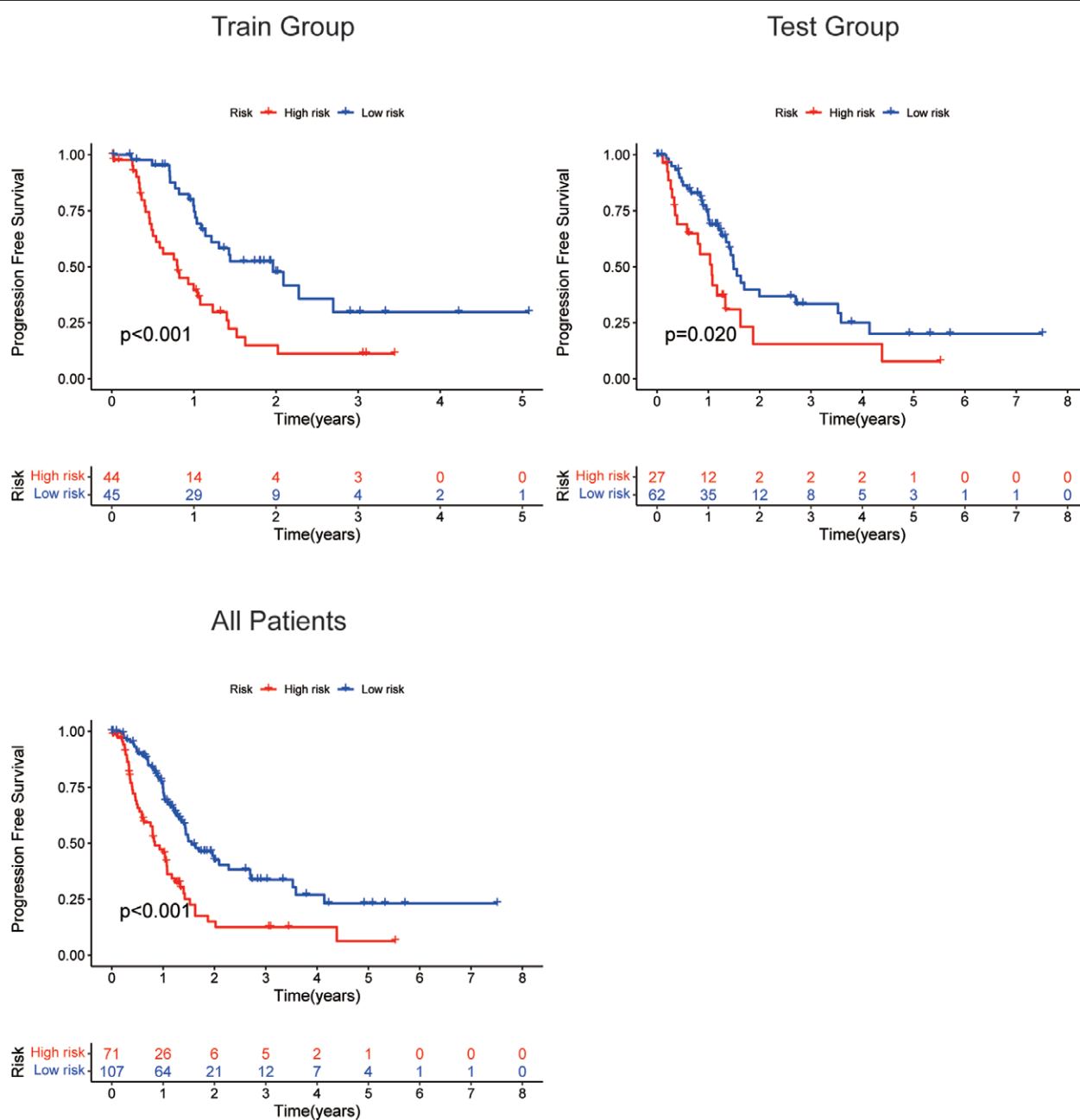


Figure 8. The Kaplan–Meier curves depicting the progress free survival (PFS) between high-risk and low-risk groups in all patients. PFS = progression free survival.

Of 251 compounds, 10 had different IC50 values different between the risk groups. Among these, GSK-650394 and pyrimethamine had greater efficacy in high-risk patients (Fig. 17) and Amuvatini, EHT1864, KIN001-135, tamoxifen, TL-1-85, TL-2-105, YM201636, and quizartinib (AC220) had greater efficacy in low-risk patients (Fig. 18).

4. Discussion

Pancreatic adenocarcinoma is a type of digestive tract tumor that is prone to invasion and metastasis in the early stages and has a high degree of malignancy. Although there has been progress in the development of treatments for pancreatic adenocarcinoma, there has yet to be a breakthrough treatment, and the options remain unsatisfactory. The tumor node metastasis staging system is useful for assessment of tumor prognosis. However, there may be different responses to treatment and prognoses between

patients despite being classified the same.^[23,24] It is therefore important to study the biological behavior of pancreatic adenocarcinomas and identify tumor prognostic markers and targets. lncRNAs are advantageous because of their increased accuracy in predicting risk. In 2022, Tsvetkov et al^[10,11] identified a copper-dependent mechanism of controlled cell death associated with mitochondrial respiration, which they named cuproptosis. Excessive intracellular copper is transported via ionophores to the mitochondria and binds to the lipoacylated proteins of the TCA cycle. This results in aggregation of lipoacylated proteins and loss of iron-sulfur cluster proteins, inducing proteotoxic stress and leading to cell death. In addition, FDX1 has been identified as an important gene in cuproptosis. This study also determined which cells are more susceptible to cuproptosis and found that these cells have dual functions in the development and treatment of tumors. Thus, elucidating the mechanism of cuproptosis may aid in developing new therapeutic strategies.

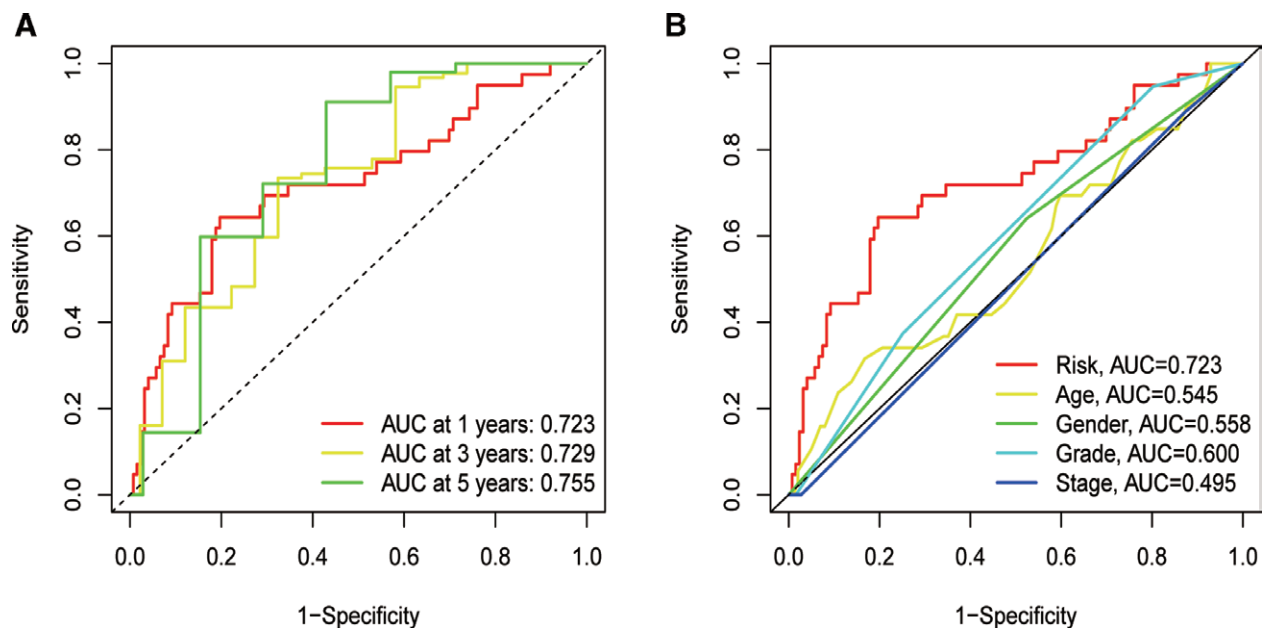


Figure 9. 1, 3, 5 years ROC curve and clinical ROC curve verify the prognostic accuracy of the risk scores in all patients. ROC = receiver operating characteristic.

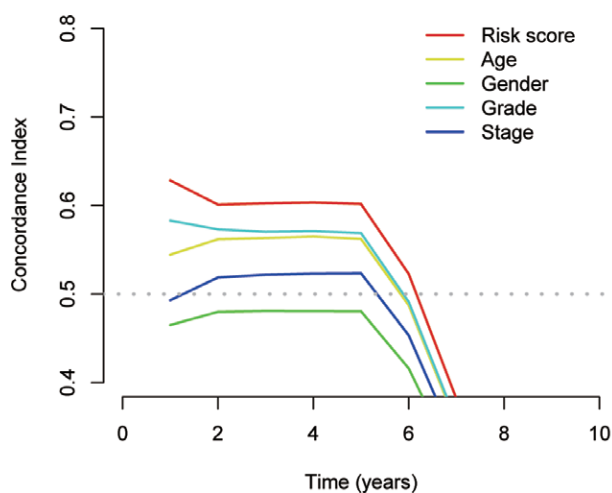


Figure 10. The consistency index (C-index) shows that the performance of this prognostic model in evaluating survival prediction is better than other clinical characters. C-index = consistency index.

Currently, there is a limited number of studies on cuproptosis-associated lncRNAs; thus, in this study we examine the relationship between cuproptosis-associated lncRNAs and pancreatic adenocarcinoma.

Through Pearson correlation, Lasso regression, and univariate and multivariate COX regression analyses, 6 characteristic cuproptosis-associated lncRNAs were obtained: AL121772.1, CASC19, AC005332.6, AC109322.2, AC017048.3, and Z97832.2. We used these lncRNAs to construct a pancreatic adenocarcinoma risk prediction model. Among them, AC005332.6, Z97832.2 were protective factors, while AL121772.1, CASC19, AC109322.2, and AC017048.3 were risk factors. Prior research has shown that AL121772.1 promotes the formation of the plasma membrane, which may promote pancreatic adenocarcinoma cell growth and metastasis.^[25,26] Studies have shown that CASC19 can promote pancreatic adenocarcinoma progression by upregulating E2F7 expression.^[27] AC005332.6 is involved in pyroptosis and ferroptosis in pancreatic adenocarcinoma cells.^[28,29] According to the available literature, no study

has shown that AC109322.2, AC017048.3, and Z97832.2 are associated with pancreatic cancer development; this study provides the first evidence that these 3 lncRNAs are involved in the cuproptosis pathway in pancreatic adenocarcinoma.

In this study, the model ROC curve and C-index demonstrate that the risk score successfully predicted the pancreatic adenocarcinoma patients prognoses at 1, 3, and 5 years, and was consistent. Kaplan–Meier analysis revealed higher OS and PFS in low risk than high risk patients. Moreover, the model showed reliable prognosis predictions across different clinical groups, indicating its potential for widespread use. More importantly, the clinical ROC curve demonstrates that the risk prediction model had higher accuracy and clinical value than other tumor node metastasis staging systems. In conclusion, this risk-prediction model is a sensitive and specific prognostic indicator for pancreatic adenocarcinoma.

Functional enrichment analysis revealed enriched DEGs pertaining to immune-related functions that were involved in the composition of immunoglobulin complexes and T-cell receptor complexes, amongst others. At the molecular level, DEGs are related to antigen-binding. It is well known that lncRNAs are critical players in various types of cancer and the tumor immune microenvironment.^[30–32] The correlation between the proposed 6 characteristic cuproptosis-associated lncRNAs and immune function was investigated using ssGSEA. The categories of T_cell_co – inhibition, checkpoint, and T_cell_co – stimulation had greater abundance among the low-risk group. Immune checkpoint inhibitors (ICIs) have increasingly been used in cancer treatment with the advent of immunotherapy; these are different from other therapeutic methods and mainly activate T cells, blocking the pathway of immune suppression, so that T cells can function effectively. T-cell memory can allow T cells to continuously recognize and attack tumors, thus greatly reducing the rate of tumor recurrence. This suggests that utilizing T-cell memory may be a strategy for achieving long-term control of the disease.^[33]

TMB quantifies the somatic mutations in the whole genome after accounting for germline DNA variants; it specifically is the amount of insertion-deletion mutations and substitutions per million bases in the exon coding region in tumor tissue. Mutations in somatic cells can lead to the production of neoantigens, which the immune system recognize as non-self-antigens, activating T cells and eliciting an immune response. Melanoma

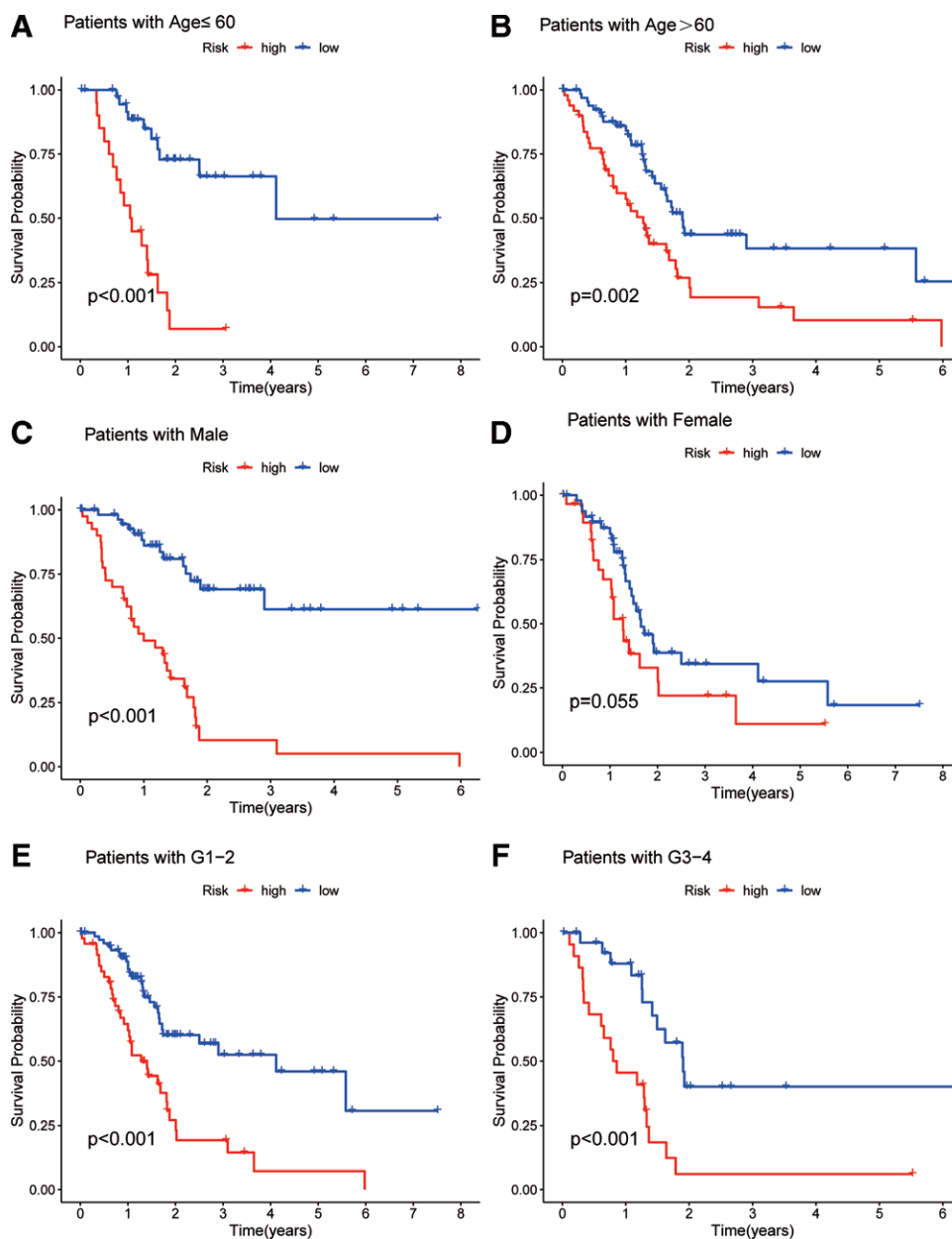


Figure 11. Stratified survival analysis. (a–b) Stratified by age. (c–d) Stratified by Gender. (e–f) Stratified by Grade.

and lung cancer patients who respond well to ICIs tend to have a higher TMB.^[34] The effect of ICIs on the TMB has been demonstrated in clinical studies.^[35] In addition, a growing body of literature has utilized a TIDE model, which is a validated computational framework used for immunotherapy prediction. This study determined that high risk patients have higher TMB than low risk patients, and TIDE scores were inversely related to risk scores, suggesting that high risk patients responded better to ICIs while the low risk group was more prone to immune evasion.

We also determined that patients with high TMB had lower survival rates. The probability of survival was highest in low-risk patients with low TMB, followed by all patients with high TMB, while the probability of survival was lowest in high risk patients with low TMB. This may be because pancreatic adenocarcinoma patients with high TMB, despite their response to ICIs monotherapy, represent < 1% of all pancreatic adenocarcinoma patients.^[36] Pancreatic adenocarcinoma is an immunosilent tumor with a lack of effector T-cell infiltration; it is therefore

unable to exploit the anti-tumor response of ICIs.^[37] This property of pancreatic adenocarcinoma is due in part to the fact that the tumor has low mutational load or neoantigen expression, with very weak immunogenicity and inability to induce activation of effector T cells.^[38] Because of its rich connective tissue stroma, pancreatic adenocarcinoma can impede T cell entry into the tumor and limit drug delivery.^[39] In addition, the pancreatic adenocarcinoma microenvironment is immunosuppressive; a large number of immunosuppressive cells infiltrate, making T-cell activation difficult, which is also an important reason for the inefficacy of ICIs against this type of cancer.^[40] Current evidence suggests that combination therapy with ICIs is the most promising to compensate for the deficiencies of ICIs and have anti-tumor effects.

Therefore, we calculated the IC50 of each sample and compared drug sensitivities of the risk groups to identify potential drugs for treating pancreatic adenocarcinoma patients and evaluate the effect of drug treatment. GSK-650394 and pyrimethamine had greater efficacy in the high-risk group.

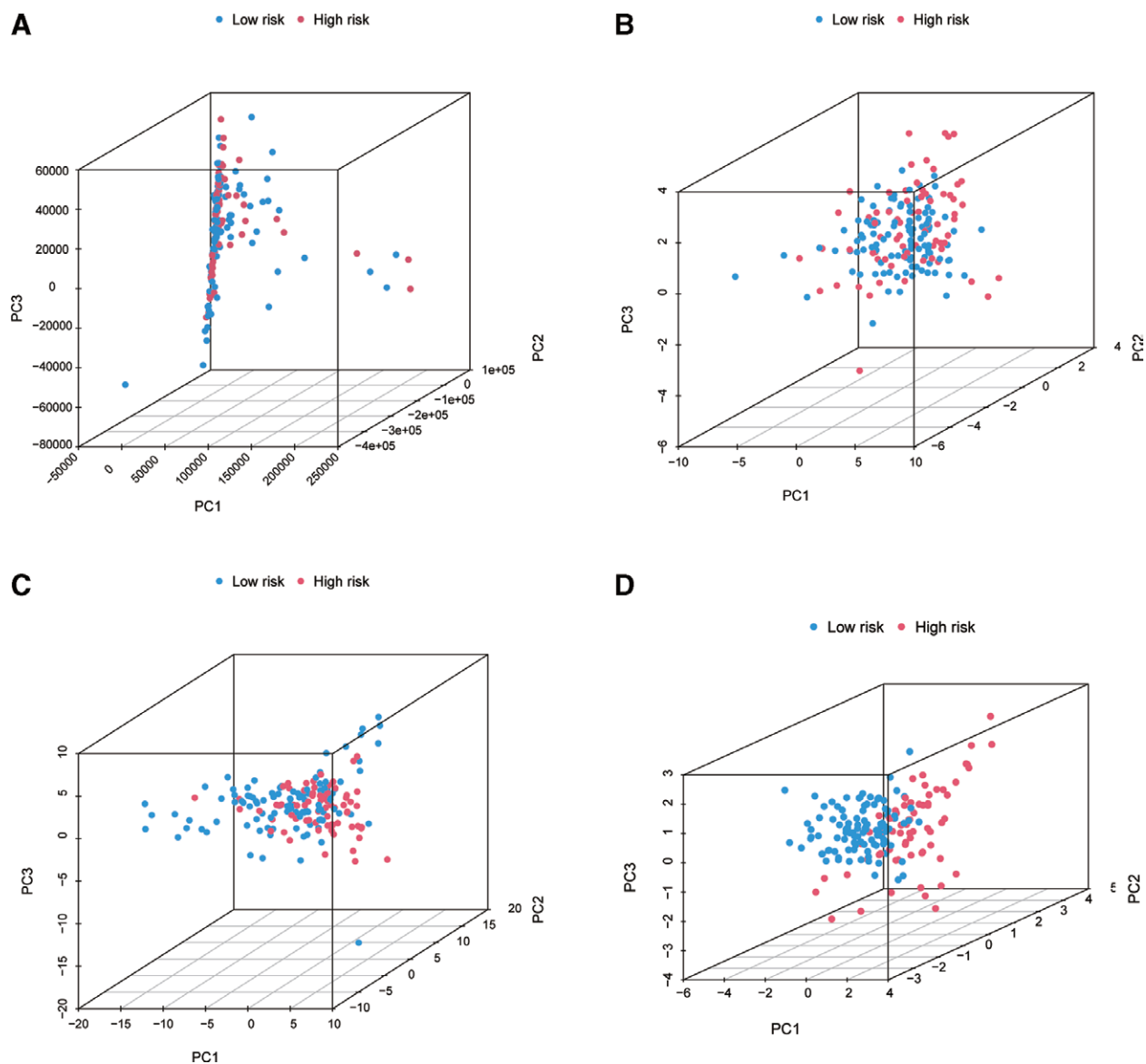


Figure 12. The principal component analysis (PCA). (a) The expression of all examined genes, (b) cuproptosis associated genes, (c) cuproptosis-associated LncRNAs, and (d) the 6 LncRNAs of the prognostic model. LncRNA = long non-coding RNA, PCA = principal component analysis.

Amuvatinib, EHT1864, KIN001-135, tamoxifen, TL-1-85, TL-2-105, YM201636, and quizartinib had greater efficacy in the low-risk group. GSK - 650394 is a type of SGK1 inhibitor, and research has shown that GSK-650394 can inhibit SGK1 kinase activity, thereby activating N-myc downstream regulatory gene 1 (NDRG1), which suppresses metastasis and contributes to the inhibition of various oncogenic signaling pathways.^[41] Pyrimethamine is a classic anti-parasitic drug. Many studies have shown that pyrimethamine also has anti-cancer activity in ovarian cancer, breast cancer, and chronic myelogenous leukemia, but there are no such reports in pancreatic adenocarcinoma.^[42-44] Amuvatinib is a tyrosine kinase inhibitor that suppresses mutant c-Kit, c-Met, c-RET, Flt3, and PDGFR α . It is also a DNA repair inhibitor that targets the RAD51-mediated DNA double-stranded break repair. Thus, the repair of DNA damage is disrupted, and anti-tumor activity is exerted.^[45,46] Mita et al showed that amuvatinib was well-tolerated adjuvant to carboplatin, carboplatin/etoposide, and paclitaxel and it exhibited anti-tumor activity in small and non-small cell lung cancer (SCLC and NSCLC).^[47] Tamoxifen

is a selective agonist of estrogen used for ER-positive breast cancer with estrogen-like effects and it can prevent chromosomal gene activation inhibit tumor cell growth. Xie et al^[48] determined that tamoxifen had cytotoxic effects on pancreatic adenocarcinoma cells regardless of hormone receptor status. Noriko et al^[49] showed that tamoxifen combined with romildesine could induce senescence in pancreatic adenocarcinoma cells by downregulating FOXM1 expression and inducing reactive and lipid peroxidation. Quezatinib, an inhibitor of FMS-like tyrosine kinase 3 (FLT3), selectively targets FLT3, which is mainly used for relapsed or refractory FLT3-ITD acute myeloid leukemia (AML).^[50] All-trans retinoic acid (ATRA) can induce apoptosis in various cells including epithelial cells, lymphocytes, and a variety of tumor cells.^[51,52] The clinical efficacy of the above 5 drugs in conjunction with ICIs for treating patients with pancreatic adenocarcinoma must be explored further in prospective experiments. The remaining 5 drugs are still in in vitro studies or early clinical trials, and their therapeutic effects on pancreatic adenocarcinoma require further investigation.

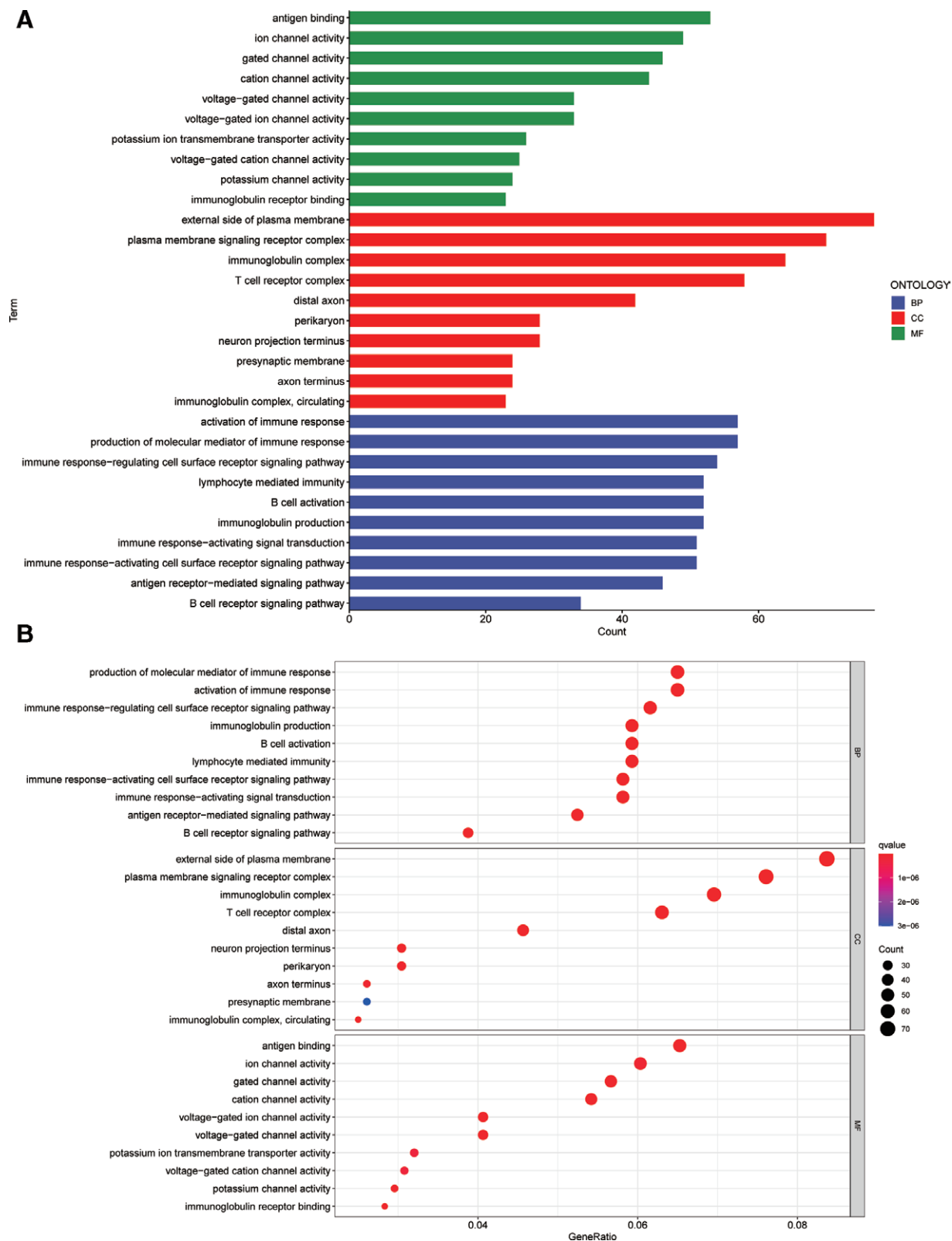


Figure 13. Analysis of GO enrichment. GO = gene ontology.

5. Conclusion

This study presents a risk prediction model of cuproptosis-associated lncRNAs, which can stably and effectively predict the prognosis pancreatic adenocarcinoma patients, provides a reference

for clinicians to aid in formulating treatment approaches, and may provide some insights for future research on the relationship between lncRNAs and cuproptosis. Furthermore, these results may aid in the development of therapeutic drugs for pancreatic adenocarcinoma.

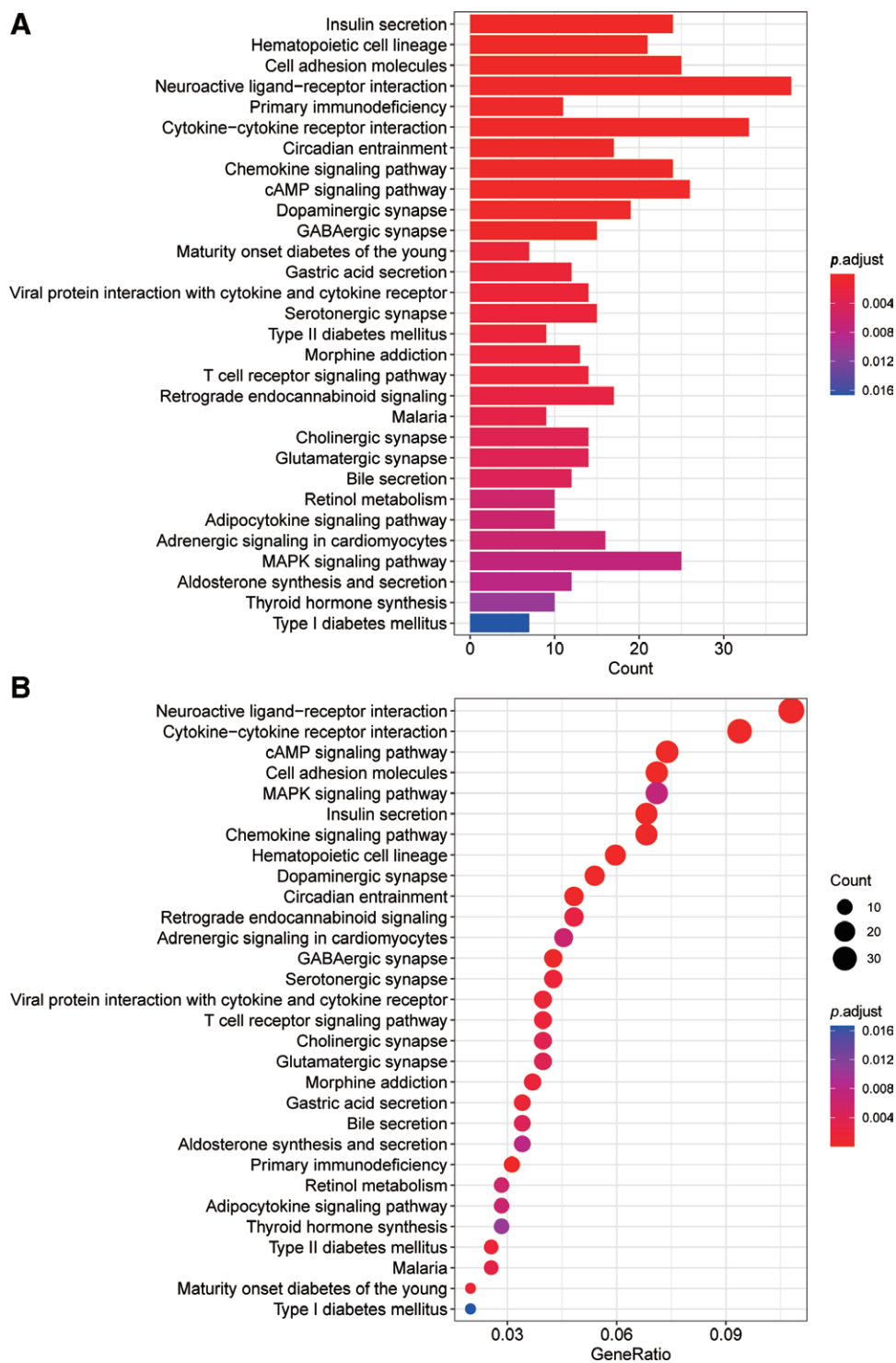


Figure 14. Analysis of KEGG pathways enrichment. KEGG = Kyoto encyclopedia of genes and genomes.

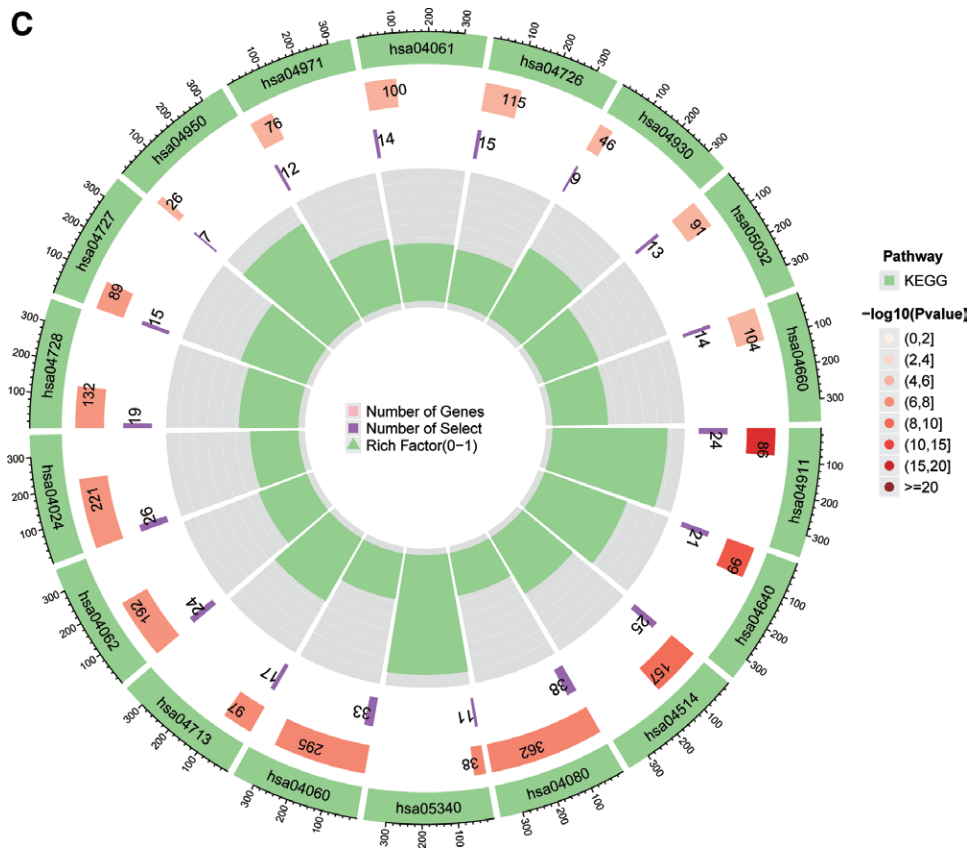


Figure 14. Continued

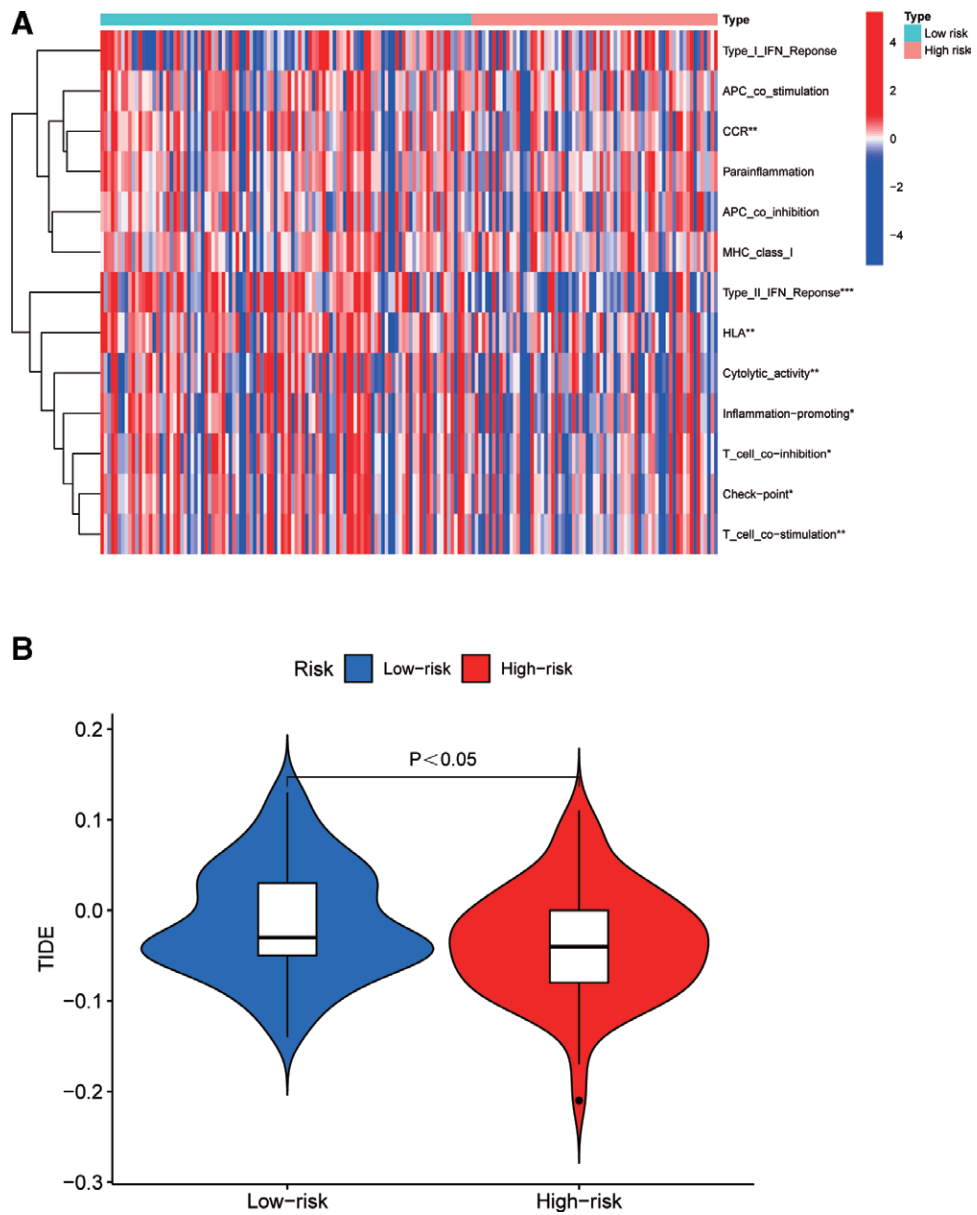


Figure 15. (a) GSVAs of immune associated functions between high-risk and low-risk groups. (b) TIDE between the high- and low-risk groups. TIDE = tumor immune dysfunction and exclusion. GSVAs = gene set variation analysis.

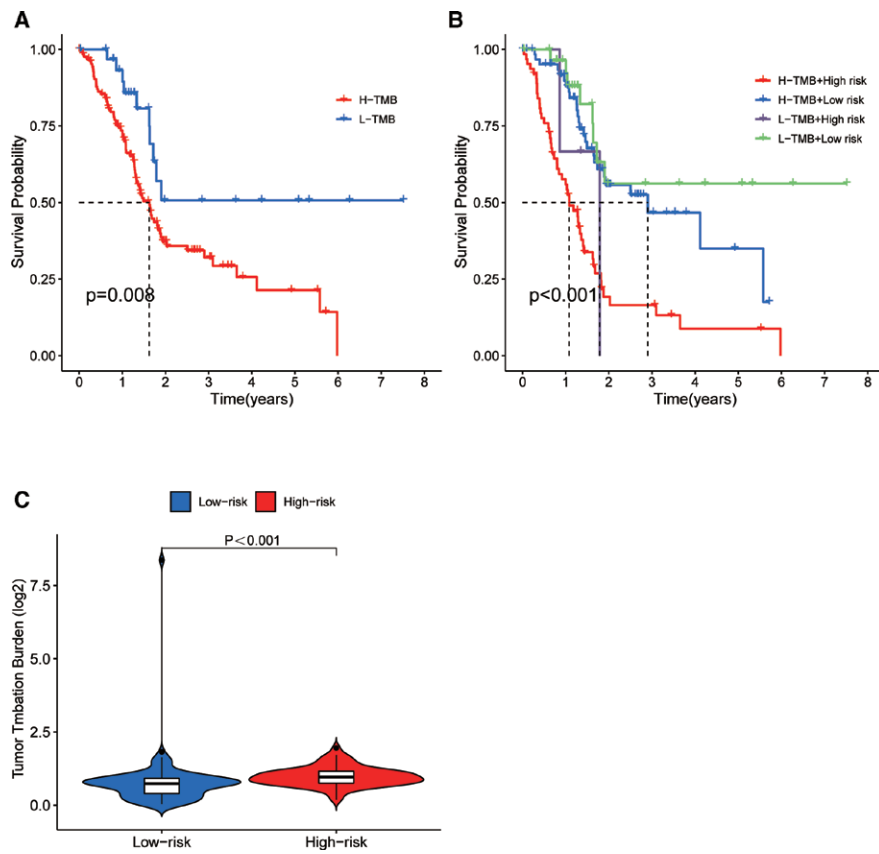


Figure 16. (a) The K-M curves of H-TMB patients and L-TMB patients. (b) The K-M curves of H-TMB patients and L-TMB patients between the high- and low-risk groups. (c) Violin plot showing the difference of TMB between the high- and low-risk groups. TMB = tumor mutation burden.

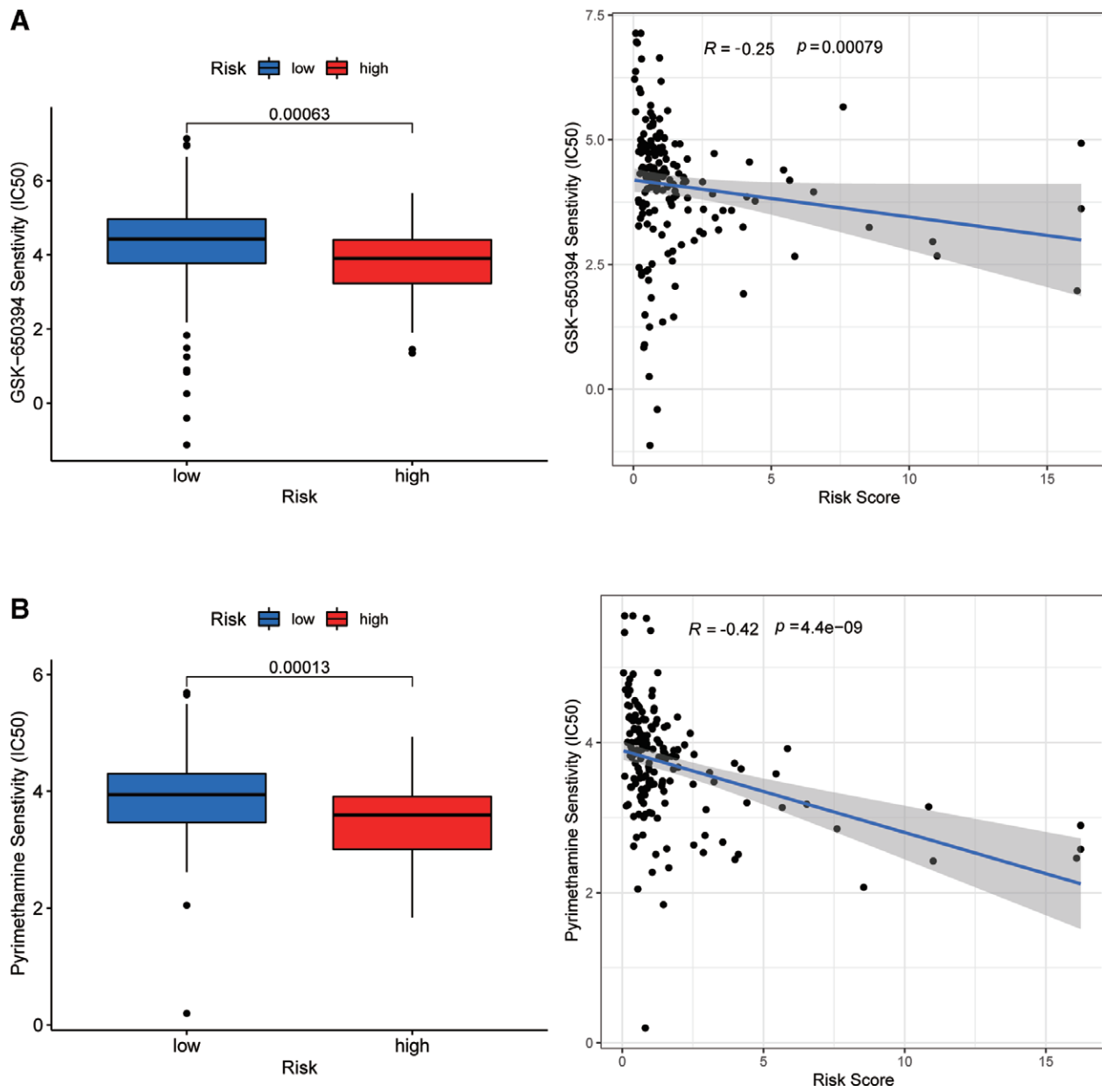


Figure 17. Drugs that may be effective for high-risk group.

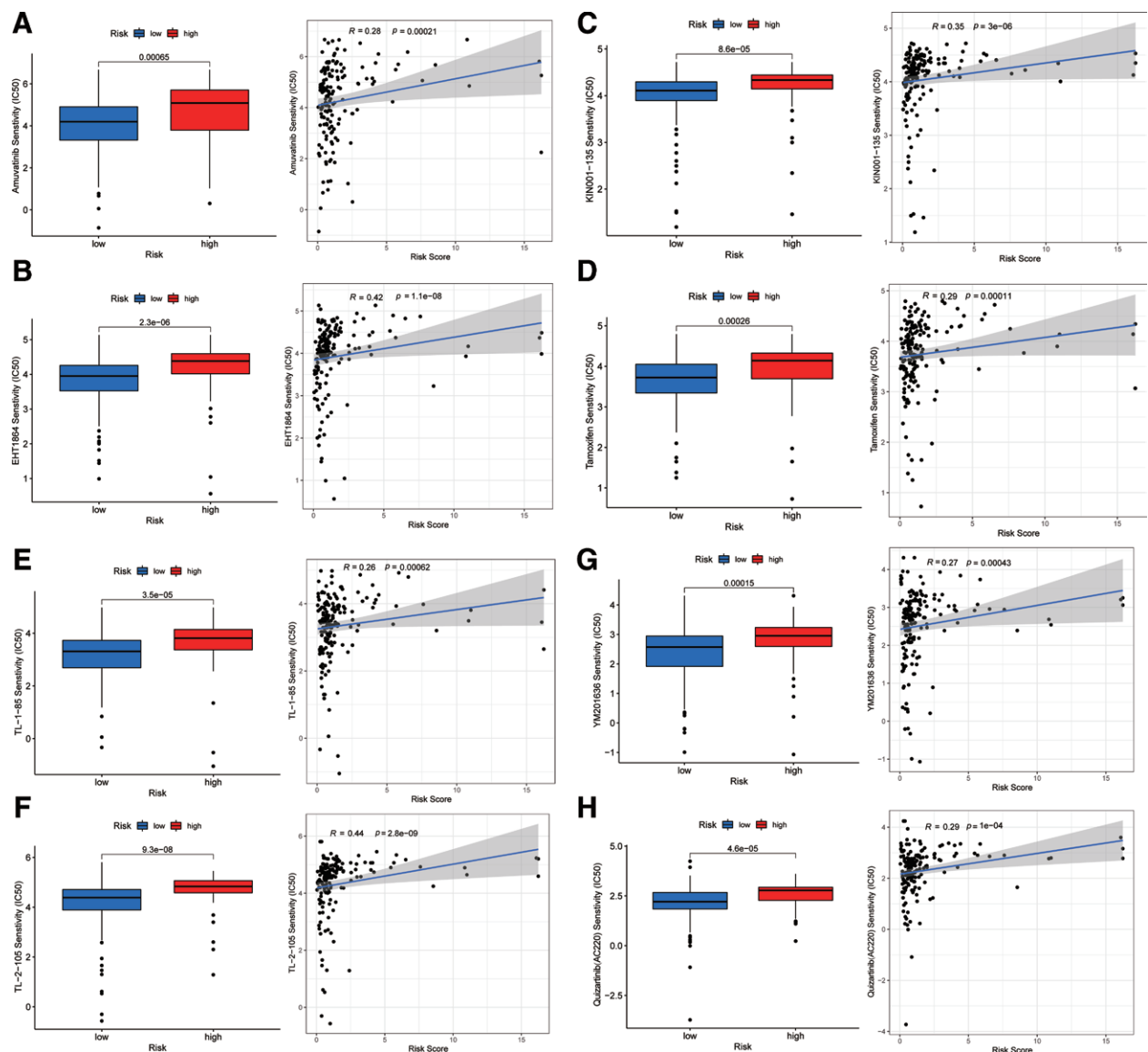


Figure 18. Drugs that may be effective for low-risk group.

Acknowledgment

We would like to thank Editage (www.editage.cn) for English language editing.

Author contributions

Data curation: Wenguang Cui.

Investigation: Wenguang Cui.

Methodology: Yaling Wang.

Project administration: Yaling Wang.

Writing – original draft: Wenguang Cui, Jianhong Guo, Zepeng Zhang.

Writing – review & editing: Wenguang Cui.

References

- [1] Siegel RL, Miller KD, Wagle NS, et al. Cancer statistics, 2022. *CA Cancer J Clin.* 2022;72:7–33.
- [2] Miller KD, Ortiz AP, Pinheiro PS, et al. Cancer statistics for the US Hispanic/Latino population, 2021. *CA Cancer J Clin.* 2021;71:466–87.
- [3] Chen W, Zheng R, Baade PD, et al. Cancer statistics in China, 2015. *CA Cancer J Clin.* 2016;66:115–32.

- [4] Cai H, An Y, Chen X, et al. Epigenetic inhibition of miR-663b by long non-coding RNA HOTAIR promotes pancreatic cancer cell proliferation via up-regulation of insulin-like growth factor 2. *Oncotarget.* 2016;7:86857–70.
- [5] Sun J, Zhang Y. LncRNA XIST enhanced TGF- β 2 expression by targeting miR-141-3p to promote pancreatic cancer cells invasion. *Biosci Rep.* 2019;39:BSR20190332.
- [6] Li H, Wang X, Wen C, et al. Long noncoding RNA NORAD, a novel competing endogenous RNA, enhances the hypoxia-induced epithelial-mesenchymal transition to promote metastasis in pancreatic cancer. *Mol Cancer.* 2017;16:169.
- [7] Zhao L, Sun H, Kong H, et al. The Lncrna-TUG1/EZH2 axis promotes pancreatic cancer cell proliferation, migration and EMT phenotype formation through sponging Mir-382. *Cell Physiol Biochem.* 2017;42:2145–58.
- [8] Lu X, Fang Y, Wang Z, et al. Downregulation of gas5 increases pancreatic cancer cell proliferation by regulating CDK6. *Cell Tissue Res.* 2013;354:891–6.
- [9] Cobine PA, Moore SA, Leary SC. Getting out what you put in: Copper in mitochondria and its impacts on human disease. *Biochim Biophys Acta Mol Cell Res.* 2021;1868:118867.
- [10] Tsvetkov P, Detappe A, Cai K, et al. Mitochondrial metabolism promotes adaptation to proteotoxic stress. *Nat Chem Biol.* 2019;15:681–9.
- [11] Tsvetkov P, Coy S, Petrova B, et al. Copper induces cell death by targeting lipoylated TCA cycle proteins. *Science.* 2022;375:1254–61.

- [12] Zhang G, Sun J, Zhang X. A novel Cuproptosis-related lncRNA signature to predict prognosis in hepatocellular carcinoma. *Sci Rep.* 2022;12:11325.
- [13] Xu M, Mu J, Wang J, et al. Construction and validation of a cuproptosis-related lncRNA signature as a novel and robust prognostic model for colon adenocarcinoma. *Front Oncol.* 2022;12:961213.
- [14] Ma S, Zhu J, Wang M, et al. A cuproptosis-related long non-coding RNA signature to predict the prognosis and immune microenvironment characterization for lung adenocarcinoma. *Transl Lung Cancer Res.* 2022;11:2079–93.
- [15] Han J, Hu Y, Liu S, et al. A newly established cuproptosis-associated long non-coding RNA signature for predicting prognosis and indicating immune microenvironment features in soft tissue sarcoma. *J Oncol.* 2022;2022:18489387–27.
- [16] Yu G, Wang LG, Han Y, et al. clusterProfiler: an R package for comparing biological themes among gene clusters. *OMICS J Integr Biol.* 2012;16:284–7.
- [17] Geeleher P, Cox N, Huang RS. pRRophetic: an R package for prediction of clinical chemotherapeutic response from tumor gene expression levels. *J PloS one.* 2014;9:e107468.
- [18] R Core Team. R: A language and environment for statistical computing. Austria: R Foundation for Statistical Computing, Vienna. 2020. URL <https://www.R-project.org/>.
- [19] Li J, Chen S, Liao Y, et al. Arecoline is associated with inhibition of cuproptosis and proliferation of cancer-associated fibroblasts in oral squamous cell carcinoma: a potential mechanism for tumor metastasis. *Front Oncol.* 2022;12:925743.
- [20] Wang Y, Zhang L, Zhou F. Cuproptosis: a new form of programmed cell death. *Cell Mol Immunol.* 2022;19:867–8.
- [21] Blockhuys S, Celauro E, Hildesjö C, et al. Defining the human copper proteome and analysis of its expression variation in cancers. *Metallomics.* 2017;9:112–23.
- [22] Ge EJ, Bush AI, Casini A, et al. Connecting copper and cancer: from transition metal signalling to metalloplasia. *Nat Rev Cancer.* 2022;22:102–13.
- [23] Choi KH, Kim BS, Oh ST, et al. Comparison the sixth and seventh editions of the AJCC staging system for T1 gastric cancer: a long-term follow-up study of 2124 patients. *Gastric Cancer.* 2017;20:43–8.
- [24] Yokoyama S, Hamada T, Higashi M, et al. Predicted prognosis of patients with pancreatic cancer by machine learning. *Clin Cancer Res.* 2020;26:2411–21.
- [25] Wu E, Guo X, Teng X, et al. Discovery of plasma membrane-associated RNAs through APEX-seq. *Cell Biochem Biophys.* 2021;79:905–17.
- [26] Xie Z, Gao Y, Ho C, et al. Exosome-delivered CD44v6/C1QBP complex drives pancreatic cancer liver metastasis by promoting fibrotic liver microenvironment. *Gut.* 2022;71:568–79.
- [27] Lu T, Wei GH, Wang J, et al. lncRNA CASC19 contributed to the progression of pancreatic cancer through modulating miR-148b/E2F7 axis. *Eur Rev Med Pharmacol Sci.* 2020;24:10462–71.
- [28] Zhao K, Li X, Shi Y, et al. A comprehensive analysis of pyroptosis-related lncRNAs signature associated with prognosis and tumor immune microenvironment of pancreatic adenocarcinoma. *Front Genet.* 2022;13:899496.
- [29] Ping H, Jia X, Ke H. A novel ferroptosis-related lncRNAs signature predicts clinical prognosis and is associated with immune landscape in pancreatic cancer. *Front Genet.* 2022;13:786689.
- [30] Schwerdtfeger M, Desiderio V, Kobold S, et al. Long non-coding RNAs in cancer stem cells. *Transl Oncol.* 2021;14:101134.
- [31] Xu M, Xu X, Pan B, et al. lncRNA SATB2-AS1 inhibits tumor metastasis and affects the tumor immune cell microenvironment in colorectal cancer by regulating SATB2. *Mol Cancer.* 2019;18:135.
- [32] Silvestri G, Trotta R, Stramucci L, et al. Persistence of drug-resistant leukemic stem cells and impaired NK cell immunity in CML patients depend on MIR300 antiproliferative and PP2A-activating functions. *Blood Cancer Discov.* 2020;1:48–67.
- [33] Klebanoff CA, Gattinoni L, Restifo NP. CD8+ T-cell memory in tumor immunology and immunotherapy. *Immunol Rev.* 2006;211:214–24.
- [34] Robert C, Long GV, Brady B, et al. Nivolumab in previously untreated melanoma without BRAF mutation. *N Engl J Med.* 2015;372:320–30.
- [35] Rizvi NA, Hellmann MD, Snyder A, et al. Cancer immunology. Mutational landscape determines sensitivity to PD-1 blockade in non-small cell lung cancer. *Science.* 2015;348:124–8.
- [36] Luchini C, Bibeau F, Ligtenberg MJL, et al. ESMO recommendations on microsatellite instability testing for immunotherapy in cancer, and its relationship with PD-1/PD-L1 expression and tumour mutational burden: a systematic review-based approach. *Ann Oncol.* 2019;30:1232–43.
- [37] Clark CE, Hingorani SR, Mick R, et al. Dynamics of the immune reaction to pancreatic cancer from inception to invasion. *Cancer Res.* 2007;67:9518–27.
- [38] Steimle V, Siegrist CA, Mottet A, et al. Regulation of MHC class II expression by interferon-gamma mediated by the transactivator gene CIITA. *Science.* 1994;265:106–9.
- [39] Knudsen ES, Vail P, Balaji U, et al. Stratification of pancreatic ductal adenocarcinoma: combinatorial genetic, stromal, and immunologic markers. *Clin Cancer Res.* 2017;23:4429–40.
- [40] Sideras K, Braat H, Kwekkeboom J, et al. Role of the immune system in pancreatic cancer progression and immune modulating treatment strategies. *Cancer Treat Rev.* 2014;40:513–22.
- [41] Sahni S, Park KC, Kovacevic Z, et al. Two mechanisms involving the autophagic and proteasomal pathways process the metastasis suppressor protein, N-myc downstream regulated gene 1. *Biochim Biophys Acta Mol Basis Dis.* 2019;1865:1361–78.
- [42] Jung YY, Kim C, Ha IJ, et al. Pyrimethamine modulates interplay between apoptosis and autophagy in chronic myelogenous leukemia cells. *Int J Mol Sci.* 2021;22:8147.
- [43] Khan MW, Saadalla A, Ewida AH, et al. The STAT3 inhibitor pyrimethamine displays anti-cancer and immune stimulatory effects in murine models of breast cancer. *Cancer Immunol Immunother.* 2018;67:13–23.
- [44] Liu Y, Zhou H, Yi T, et al. Pyrimethamine exerts significant antitumor effects on human ovarian cancer cells both in vitro and in vivo. *Anticancer Drugs.* 2019;30:571–8.
- [45] Mahadevan D, Theiss N, Morales C, et al. Novel receptor tyrosine kinase targeted combination therapies for imatinib-resistant gastrointestinal stromal tumors (GIST). *Oncotarget.* 2015;6:1954–66.
- [46] Tibes R, Fine G, Choy G, et al. A phase I, first-in-human dose-escalation study of amuvatinib, a multi-targeted tyrosine kinase inhibitor, in patients with advanced solid tumors. *Cancer Chemother Pharmacol.* 2013;71:463–71.
- [47] Mita M, Gordon M, Rosen L, et al. Phase 1B study of amuvatinib in combination with five standard cancer therapies in adults with advanced solid tumors. *Cancer Chemother Pharmacol.* 2014;74:195–204.
- [48] Xie X, Wu MY, Shou LM, et al. Tamoxifen enhances the anticancer effect of cantharidin and norcantharidin in pancreatic cancer cell lines through inhibition of the protein kinase C signaling pathway. *Oncol Lett.* 2015;9:837–44.
- [49] Okuni N, Honma Y, Urano T, et al. Romidepsin and tamoxifen cooperatively induce senescence of pancreatic cancer cells through downregulation of FOXM1 expression and induction of reactive oxygen species/lipid peroxidation. *Mol Biol Rep.* 2022;49:3519–29.
- [50] Ostronoff F, Estey E. The role of quizartinib in the treatment of acute myeloid leukemia. *Expert Opin Investig Drugs.* 2013;22:1659–69.
- [51] Li M, Song S, Lippman SM, et al. Induction of retinoic acid receptor-beta suppresses cyclooxygenase-2 expression in esophageal cancer cells. *Oncogene.* 2002;21:411–8.
- [52] Zhang JW, Wang JY, Chen SJ, et al. Mechanisms of all-trans retinoic acid-induced differentiation of acute promyelocytic leukemia cells. *J Biosci.* 2000;25:275–84.